ESC HEART FAILURE
ESC Heart Failure 2025; **12**: 1416–1426
Published online 9 December 2024 in Wiley Online Library (wileyonlinelibrary.com) **DOI:** 10.1002/ehf2.15159

ORIGINAL ARTICLE

SPARCL1 and NT-proBNP as biomarkers of right ventricular-to-pulmonary artery uncoupling in pulmonary hypertension

Oliver Dörr[1,2,3]*, Stanislav Keranov[1], Paulina van Wickern[1], Holger Nef[4], Christian Hamm[1,3], Pascal Bauer[1], Christian Troidl[1,3], Samuel Sossalla[1,3,5], Sandra Voss[3,5], Christoph Liebetrau[2,3], Manuel J. Richter[6], Henning Gall[6], Werner Seeger[6], Ardeschir Ghofrani[6], Athiththan Yogeswaran[6] and Khodr Tello[6]

[1]*Department of Cardiology and Angiology, University of Giessen, Giessen, Germany;* [2]*Cardioangiological Center Bethanien (CCB), Frankfurt, Germany;* [3]*German Center for Cardiovascular Research (DZHK) Partner Site Rhine-Main, Bad Nauheim, Germany;* [4]*Department of Cardiology, Heart and Vascular Center Bad Segeberg, Bad Segeberg, Germany;* [5]*Department of Cardiology, Kerckhoff Heart and Lung Center, Bad Nauheim, Germany; and* [6]*Department of Internal Medicine, Justus-Liebig-University Giessen, Universities of Giessen and Marburg Lung Center (UGMLC), Institute for Lung Health (ILH), Cardio-Pulmonary Institute (CPI), Member of the German Center for Lung Research (DZL), Giessen, Germany*

Abstract

Aims SPARCL1 was recently identified as a biomarker of right ventricular (RV) maladaptation in patients with pulmonary hypertension (PH), and N-terminal pro-brain natriuretic protein (NT-proBNP) is an established biomarker of RV failure in PH. The present study investigated whether NT-proBNP and SPARCL1 concentrations are associated with load-independent parameters of RV function and RV-to-pulmonary artery (RV–PA) coupling as measured using invasive pressure–volume (PV) loops in the RV.

Methods SPARCL1 and NT-proBNP were measured in the plasma of patients with idiopathic pulmonary artery hypertension (IPAH, $n = 73$). Participants without LV or RV abnormalities served as controls ($n = 28$). All patients underwent echocardiography and right heart catheterization with invasive PV loop measurements.

Results Our cohort had more females with IPAH than the control group (64% vs. 35%; $P = 0.01$) and was older [69 (interquartile range, IQR 57–76) vs. 51 (IQR 35–62) years; $P < 0.001$]. SPARCL1 and NT-proBNP levels were significantly higher in patients with IPAH as compared with controls ($P < 0.0001$). Patients with IPAH and maladaptive RV remodelling had higher SPARCL1 and NT-proBNP concentrations than those with adaptive RV remodelling ($P < 0.01$). Both SPARCL1 and NT-proBNP were good predictors of maladaptive RV remodelling in receiver operating characteristic analysis [area under the curve (AUC) ($AUC_{SPARCL1} = 0.75$, $AUC_{NT\text{-}proBNP} = 0.72$, $P = 0.36$ for $AUC_{SPARCL1}$ vs. $AUC_{NT\text{-}proBNP}$]. The combined predictive value of SPARCL1 and NT-proBNP (AUC 0.78, $P < 0.001$) for maladaptive RV was numerically higher than that of either SPARCL1 or NT-proBNP alone ($P = 0.16$ for $AUC_{SPARCL1\ +\ NT\text{-}proBNP}$ vs. $AUC_{NT\text{-}proBNP}$ and $P = 0.18$ for $AUC_{SPARCL1\ +\ NT\text{-}proBNP}$ vs. $AUC_{SPARCL1}$). SPARCL1 showed numerically a tendency for a better predictive power than NT-proBNP for parameters of early maladaptive RV remodelling such as RV ejection fraction $< 50\%$ ($AUC_{SPARCL1} = 0.77$, $AUC_{NT\text{-}proBNP} = 0.67$, $P = 0.06$ for $AUC_{SPARCL1}$ vs. $AUC_{NT\text{-}proBNP}$), RV end-diastolic diameter > 42 mm ($AUC_{SPARCL1} = 0.72$, $AUC_{NT\text{-}proBNP} = 0.65$, $P = 0.19$ for $AUC_{SPARCL1}$ vs. $AUC_{NT\text{-}proBNP}$) and RV end-systolic volume index RVESVI > 31 mL/m^2 ($AUC_{SPARCL1} = 0.78$, $AUC_{NT\text{-}proBNP} = 0.71$, $PP = 0.10$ for $AUC_{SPARCL1}$ vs. $AUC_{NT\text{-}proBNP}$).

Conclusions SPARCL1 and NT-proBNP are good predictors of maladaptive RV remodelling and RV–PA uncoupling in IPAH patients. SPARCL1 may be a better predictor of early maladaptive RV remodelling than NT-proBNP.

Keywords RV–PA coupling; PV loops; Ees/Ea; RV dysfunction; RV remodelling

Received: 1 June 2024; Revised: 10 October 2024; Accepted: 24 October 2024
**Correspondence to: Oliver Dörr, Department of Cardiology and Angiology, University of Giessen, Klinikstr. 33, 35392 Giessen, Germany.*
Email: oliver.doerr@innere.med.uni-giessen.de
Oliver Dörr and Stanislav Keranov contributed equally to this work.
Athiththan Yogeswaran and Khodr Tello contributed equally to this work.

Introduction

In idiopathic pulmonary arterial hypertension (IPAH), the adaptation of the right ventricle (RV) to the chronic pressure overload caused by increased resistance in the precapillary pulmonary vasculature is the key prognostic determinant. Progressively increasing afterload often leads to maladaptive RV remodelling, resulting in RV-to-pulmonary artery (RV–PA) uncoupling and right heart failure.[1]

Pressure–volume (PV) catheterization is the gold standard for the measurement of load-independent systolic and diastolic function as well as RV–PA coupling.[2] RV–PA measurements provide the best assessment of intrinsic changes in RV myocardium associated with maladaptive RV remodelling; however, such measurements are made by an invasive and time-consuming procedure that cannot easily be implemented in the daily clinical routine. Hence, it is of paramount importance to develop new methods for the non-invasive detection of RV maladaptation in the setting of pulmonary arterial hypertension (PAH) to improve therapeutic approaches and outcomes. Current concepts involve the development of a panel of non-invasive tools such as biomarkers and echocardiography.

N-terminal pro-brain natriuretic peptide (NT-proBNP) is currently the only established biomarker of heart failure recommended by the latest ESC/ERS guidelines for the diagnosis and treatment of pulmonary hypertension (PH).[3] It is released by cardiomyocytes in response to RV wall stress,[4] and its levels are closely associated with RV load, as confirmed by numerous studies.[5] However, little is known about the association of NT-proBNP with load-independent, PV loop-derived RV parameters in patients with PAH. Furthermore, NT-proBNP is not a specific biomarker of RV remodelling, as it is also elevated in numerous left ventricular (LV) pathologies.

SPARC-like protein 1 (SPARCL1, also known as Hevin or SC1) is a matricellular protein involved in pathological myocardial remodelling under chronic pressure overload.[6,7] In a recently published pilot study, our research group identified SPARCL1 as a potential specific biomarker of maladaptive RV remodelling in patients with IPAH and chronic thromboembolic PH.[8] However, in this study, adaptive and maladaptive RV remodelling were defined by load-dependent echocardiographic parameters and not by load-independent PV loop measurements.

Therefore, the main goal of the current study was to assess the association of NT-proBNP and SPARCL1 with load-independent PV loop parameters of RV systolic and diastolic function and RV–PA coupling in patients with PAH to obtain new insights on their utility as biomarkers of RV maladaptive remodelling.

Patients and methods

Study population

Patient data and blood samples of IPAH patients who were prospectively enrolled in the Giessen Pulmonary Hypertension Registry between January 2016 and April 2021 were used in this retrospective analysis.[9] All patients provided written informed consent for their participation in the study, and approval of the Institutional Review Board of the University of Giessen (99/13) was obtained. The investigation conforms to the principles outlined in the Declaration of Helsinki.

Inclusion criteria

Patients who were clinically diagnosed with IPAH ($n = 73$) were included if they fulfilled all of the following criteria: age $>$ 18 years, mean pulmonary artery pressure (mPAP) $\geq$ 20 mmHg, pulmonary artery wedge pressure $\leq$ 15 mmHg, LV ejection fraction (LVEF) $\geq$ 50%, LV end-diastolic diameter (LVEDd) $<$ 56 mm, no relevant pathology of the aortic and mitral valve and no LV hypertrophy [end-diastolic interventricular septum thickness (IVSd) $\leq$ 13 mm]. The number of patients with incident IPAH was 38 (52%).

Samples from a cohort without any RV or LV abnormalities were used as controls.

Classification of patients with IPAH

Adaptive RV remodelling was defined as low or low-to-intermediate risk of 1 year mortality according to the three-strata model of the ESC/ERS guidelines for the diagnosis and treatment of PH.[3] Thus, the following determinants of prognosis and cut-offs were used to define adaptive RV remodelling: right atrium (RA) area $\leq$ 26 cm^2, ratio of tricuspid annular plane systolic excursion to pulmonary artery systolic pressure (TAPSE/PASP) $\geq$ 0.32, TAPSE $\geq$ 20 mm, RV ejection fraction (RVEF) $\geq$ 37%, RV end-systolic volume index (RVESVI) determined by 3D echocardiography $\leq$ 40 mL/m^2, RA pressure $\leq$ 11 mmHg, cardiac index (CI) $\geq$ 2.4 l/min/m^2,

Maladaptive RV remodelling was defined as high or intermediate-to-high risk of 1 year mortality according to the three-strata model of the ESC/ERS guidelines for the diagnosis and treatment of PH.[3] Thus, the following determinants of prognosis and cut-offs were used to define maladaptive RV remodelling: RA area $>$ 18 cm^2, TAPSE/PASP $<$ 0.32, TAPSE $<$ 20 mm, RVEF $<$ 37%, RVESVI determined by 3D echocardiography $>$ 40 mL/m^2 and CI $<$ 2.4 L/min/m^2.

Laboratory assessments

Venous blood samples were collected in EDTA tubes (Monovette, Saarstedt, Nümrecht, Germany) for the determination of SPARCL1 and NT-proBNP concentrations. Plasma was processed immediately and frozen at −80°C until assay. SPARCL1 levels were determined using an enzyme-linked immunosorbent assay (Human SPARC Like Protein 1 ELISA, abbexa, Cambridge, UK). NT-proBNP levels were measured with chemiluminescent microparticle immunoassay (CMIA Architect, Abbot diagnostics, Illinois, USA).

Transthoracic echocardiography

All patients underwent transthoracic two-dimensional echocardiography using commercially available ultrasound systems (EPIQ 7, Philips Ultrasound Systems, Koninklijke Philips N.V., Amsterdam, the Netherlands). Left and right ventricular assessment was performed as recommended by recent guidelines.[10]

Right heart catheterization

Right heart catheterization was performed via the right internal jugular vein using an 8F sheath and a standard Swan–Ganz catheter as described previously.[9,11]

Pressure–volume catheterization

A 4F PV catheter (CA-Nr 41063, CD Leycom, Zoetermeer, the Netherlands) was positioned in the RV apex (using the same 8F introducer sheath as above) under guidance of transthoracic echocardiography and analysis of online PV loops. The pressure–volume loop catheter was calibrated using magnetic resonance imaging (MRI), as previously described. Imaging was performed at 1.5 Tesla with a six-element phased array cardiac coil and a dedicated CMR protocol to generate SSFP cine sequences in multiple views. RV systolic and diastolic volumes were calculated from short-axis cine images obtained during breath hold, with measurements taken from end-diastolic and end-systolic images. Real-time beat-to-beat display of PV loops was achieved by connection to an intracardiac analyser (Inca®, CD Leycom). Single-beat measurements were each evaluated separately by two experienced examiners who were blinded to the other data and supervised by the first author. Ees was calculated using the single-beat method for the RV.[12] In brief, RV pressure–time curves were used to extrapolate isovolumetric Pmax. Ees equals (Piso − ESP)/SV, and Ea equals ESP/SV, making Ees/Ea equal to Piso/ESP − 1. Notably, we validated this approach at our centre by comparing it with multi-beat Ees, Ea and Ees/Ea. Ea was calculated as end-systolic pressure/SV.[12] RV-arterial coupling was defined as Ees/Ea. Eed was calculated as an end-diastolic pressure/volume ratio,[13] which has been shown to agree with the more rigorous diastolic elastance coefficient β calculated from a curvilinear adjustment of end-systolic and end-diastolic pressure/volume ratios.[13,14]

Statistical analysis

Continuous variables are presented as the mean ± standard deviation (SD) or median with 25th to 75th interquartile range (IQR), as appropriate. Categorical variables are expressed as numbers and percentages. Parametric distribution was assessed with the Shapiro–Wilk test. Normally distributed continuous variables were compared using the Welch two-sample *t*-test and one-way analysis of variance with Bonferroni post-hoc test. The Mann–Whitney *U* test and the Kruskal–Wallis test with Dunnett's post-hoc test were used for non-normally distributed continuous variables. Receiver operating characteristic (ROC) curve analysis was performed to assess the predictive value of SPARCL1 and NT-proBNP regarding maladaptive RV remodelling. A two-tailed P value < 0.05 was considered to indicate statistical significance. Statistical analyses were performed using SPSS Version 25.0.0 (SPSS Inc., Chicago, IL, USA).

Results

Characteristics of the study population

Clinical characteristics of patients with IPAH and controls are shown in *Table* 1. Patients with IPAH were older ($P < 0.001$) and there were more females ($P < 0.01$) and patients with NYHA ≥ III ($P < 0.001$) and arterial hypertension ($P = 0.002$) compared with the controls. These patients also had lower TAPSE ($P < 0.0001$) and TAPSE/PASP ($P < 0.0001$) as well as higher RV end-diastolic diameter (RVEDd) ($P < 0.0001$) and PASP ($P < 0.0001$) than controls. Conversely, there were no differences between the two groups in terms of LVEF, LVEDd, IVSd and LVPWd ($P > 0.05$ for all comparisons).

Patients with IPAH had higher NT-proBNP and SPARCL1 levels ($P < 0.0001$ for both comparisons) than controls (*Figure* 1). Median estimated glomerular filtration rate (eGFR) in IPAH patients was 77 mL/min/1.73 m^2 (IQR: 57–101) and for controls 92 mL/min/1.73 m^2 (IQR: 79–113, $P = 0.03$).

Table 1 Clinical characteristics.

	Controls $n = 28$	IPAH $n = 73$	P value
Female sex, *n* (%)	10 (36%)	47 (64%)	0.01
Age, years, median (IQR)	51 (35–62)	69 (57–76)	<0.001
BMI, kg/m^2, median (IQR)	26 (24–27)	25 (24–30)	0.06
NYHA ≥ III, *n* (%)	0 (0%)	40 (57%)	<0.001
Arterial hypertension, *n* (%)	4 (15%)	37 (51%)	0.002
Diabetes, *n* (%)	0 (0%)	9 (13%)	0.07
Hypercholesterolemia, *n* (%)	5 (18%)	7 (10%)	0.26
CAD, *n* (%)	3 (11%)	9 (12%)	0.87
COPD, *n* (%)	2 (7%)	8 (11%)	0.76
Stroke, *n* (%)	0 (0%)	2 (3%)	0.40
Right heart catheterization			
PASP, mmHg, median (IQR)	N/A	55 (33–79)	N/A
mPAP, mmHg, median (IQR)	N/A	35 (21–45)	N/A
PCWP, mmHg, median (IQR)	N/A	10 (7–13)	N/A
PVR, dyn s cm^{-5}, median (IQR)	N/A	296 (152–556)	N/A
CI, L/min/m^2, median (IQR)	N/A	2.69 (2.33–3.07)	N/A
RAP, mmHg, median (IQR)	N/A	7 (5–10)	N/A
PV loop measurements			
RV EDP, mmHg, median (IQR)	N/A	6 (3–9)	N/A
RV ESP, mmHg, median (IQR)	N/A	44 (29–60)	N/A
SW, mmHg mL m^{-2}, median (IQR)	N/A	2097 (1375–2958)	N/A
Tau, ms, median (IQR)	N/A	34 (28–41)	N/A
dP/dt min, mmHg/s, median (IQR)	N/A	−436 (−548 to −284)	N/A
dP/dt max, mmHg/s, median (IQR)	N/A	387 (312–470)	N/A
Eed, mmHg/mL, median (IQR)	N/A	0.19 (0.13–0.29)	N/A
Ees, mmHg/mL, median (IQR)	N/A	0.71 (0.52–0.94)	N/A
Ees/Ea ratio, median (IQR)	N/A	1.16 (0.95–1.47)	N/A
Echocardiography			
LVEF, %, median (IQR)	55 (55–60)	59 (55–62)	0.27
TAPSE, mm, median (IQR)	24 (22–25)	20 (18–23)	<0.0001
PASP, mmHg, median (IQR)	26 (22–28)	54 (32–72)	<0.0001
TAPSE/PASP, mm/mmHg, median (IQR)	0.89 (0.82–1.11)	0.41 (0.23–0.67)	<0.0001
RA area, cm^2, median (IQR)	N/A	19 (14–24)	N/A
RVEDd, mm, median (IQR)	35 (30–39)	45 (42–52)	<0.0001
IVSd, mm, median (IQR)	10 (9–11)	11 (10–11)	0.33
LVPWd, mm, median (IQR)	10 (9–11)	10 (8–10)	0.44
LVEDd, mm, median (IQR)	46 (42–50)	44 (42–48)	0.11
RV EDA, cm^2, median (IQR)	N/A	26.7 (21.1–31.0)	N/A
RV ESA, cm^2, median (IQR)	N/A	17 (13–22)	N/A
FAC, %, median (IQR)	N/A	36.2 (30.4–41.5)	N/A
RVFWS, median (IQR)	N/A	−23 (−26 - − 19)	N/A
RVGLS, median (IQR)	N/A	-19 (−22 - -16)	N/A
3D echocardiography			
RVEDV, mL, median (IQR)	N/A	131 (106–160)	N/A
RVEDVI, mL/m^2, median (IQR)	N/A	65 (54–81)	N/A
RVESV, mL, median (IQR)	N/A	74 (54–101)	N/A
RVESVI, mL/m^2, median (IQR)	N/A	38 (27–51)	N/A
RVSVI, mL/m^2, median (IQR)	N/A	27 (23–31)	N/A
RVEF, %, median (IQR)	N/A	42 (37–48)	N/A
Biomarkers			
SPARCL1, ng/mL, median (IQR)	1.74 (1.11–2.12)	3.56 (1.91–6.30)	<0.0001
NT-proBNP, pg/mL, median (IQR)	41 (25–68)	287 (70–1,391)	<0.0001
eGFR, mL/min/1.73 m^2, median (IQR)	92 (79–113)	77 (57–101)	0.03

Abbreviations: BMI, body mass index; CAD, coronary artery disease; CI, cardiac index; COPD, chronic obstructive pulmonary disease; Eed, end-diastolic elastance; Ees, end-systolic elastance; eGFR, estimated glomerular filtration rate; FAC, fractional area change; IVSd, interventricular septum diastolic diameter; LVEDd, left ventricular end-diastolic diameter; LVEF, left ventricular ejection fraction; LVPWd, left ventricular posterior wall diastolic diameter; MI, myocardial infarction; mPAP, mean pulmonary arterial pressure; NT-proBNP, N-terminal pro-brain natriuretic protein; NYHA, New York Heart Association; PASP, systolic pulmonary artery pressure; PCWP, pulmonary capillary wedge pressure; PV, pulmonary vein; PVR, pulmonary vein resistance; RA area, right atrial; RAP, right atrial pressure; RV EDA, right ventricular end-diastolic area; RV EDP, right ventricular end-diastolic pressure; RV ESA, right ventricular end-systolic area; RV ESP, right ventricular end-systolic pressure; RVEDd, right ventricular end-diastolic diameter; RVEDV, right ventricular end-diastolic volume; RVEDVI, right ventricular end-diastolic volume index; RVEF, right ventricular ejection fraction; RVESV, right ventricular end-systolic volume index; RVESVI, right ventricular end-systolic volume index; RVFWS, right ventricular free wall strain; RVGLS, right ventricular global longitudinal strain; RVSVI, right ventricular stroke volume index; SPARCL1, SPARC-like protein 1; SW, stroke work; TAPSE, tricuspid annular plane systolic excursion.

Figure 1 Plasma biomarker levels in IPAH patients and controls. (A) NT-proBNP levels. (B) SPARCL1 levels. ****$P < 0.0001$. IPAH, idiopathic pulmonary hypertension; NT-proBNP, N-terminal pro-brain natriuretic protein; SPARCL1, SPARC-like protein 1.

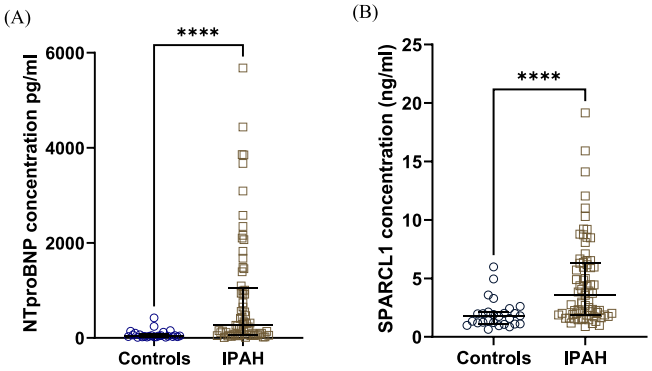

SPARCL1 and NT-proBNP levels in adaptive vs. maladaptive RV remodelling

In IPAH patients, SPARCL1 and NT-proBNP levels showed a moderate correlation with the following invasive PV loop parameters: Ees (r = 0.30, P = 0.01 for SPARCL1; r = 0.36, P = 0.01 for NT-proBNP, *Figure* S1A,B), Eed (r = 0.32, P = 0.006 for SPARCL1; r = 0.35, P = 0.002 for NT-proBNP, *Figure* S1C,D), Tau (r = 0.37, P = 0.001 for SPARCL1; r = 0.41, $P < 0.001$ for NT-proBNP, *Figure* S1E,F) and Ees/Ea (r = 0.51 for SPARCL1, $P < 0.0001$; r = 0.49, $P < 0.0001$ for NT-proBNP, *Figure* S1G,H).

Clinical characteristics of IPAH patients according to adaptive or maladaptive RV remodelling are shown in *Table* 2. There were no differences in terms of age, sex, cardiovascular risk factors, coronary artery disease, stroke, previous myocardial infarction and chronic obstructive pulmonary disease. Kidney function as measured by the eGFR was lower in maladaptive RV patients ($P < 0.001$); however, it was not substantially reduced (median in maladaptive RV: 60 mL/min/1.73 m^2, IQR: 46–71 mL/min/1.73 m^2).

There were significant differences between the two groups concerning echocardiographic and invasive parameters. In IPAH patients with adaptive RV remodelling, pulmonary parameters such as PVR and mPAP (Figure S2A) were lower than in patients with maladaptive RV remodelling ($P < 0.001$ for all comparisons). Conversely, invasive and non-invasive parameters of RV–PA coupling, Ees/Ea (Figure S2B) and TAPSE/PASP (Figure S2C), were lower in patients with maladaptive RV remodelling ($P < 0.001$ for all comparisons). Furthermore, parameters of systolic RV function, Ees (Figure S2D), RVEF (Figure S2E) and TAPSE, were lower, and parameters of diastolic RV function, Eed (Figure S2F) and Tau (Figure S2G), were higher in patients with maladaptive RV remodelling ($P < 0.01$ for all comparisons). Parameters of RV dilation, RVEDd and RVESVI (Figure S2H), were also higher in patients with maladaptive RV remodelling. Representative PV loops for patients with adaptive and maladaptive RV remodelling are included in the supplementary data (Figure S2I).

NT-pro-BNP and SPARCL1 levels were higher in IPAH patients with maladaptive RV remodelling than in those with adaptive RV remodelling (P = 0.003 for NT-proBNP, *Figure* 2A, and P = 0.001 for SPARCL1, *Figure* 2B). Patients in both subgroups with IPAH had higher SPARCL1 and NT-proBNP levels than controls (*Figure* 2, $P < 0.05$ for all comparisons).

ROC curve analysis of biomarker levels in all IPAH patients showed that both SPARCL1 (AUC 0.75, P = 0.001) and NT-proBNP (AUC 0.72, P = 0.003) were good predictors of maladaptive RV remodelling (*Figure* 3). The combined predictive value of SPARCL1 and NT-proBNP was higher than that of SPARCL1 or NT-proBNP alone (AUC 0.78, $P < 0.001$). However, comparison of the three ROC curves did not show any significant differences ($P > 0.05$ for all comparisons).

Optimal SPARCL1 and NT-proBNP cut-off values for maladaptive RV remodelling were 3.74 ng/mL (sensitivity: 81%; specificity: 66%) and 921 pg/mL (sensitivity: 62%; specificity: 79%), respectively. The combined predictive value of SPARCL1 and NT-proBNP showed two optimal peaks with equal Youden values in the ROC analysis for maladaptive RV remodelling: 0.17 (sensitivity: 87%; specificity: 63%) and 0.21 (sensitivity: 76%; specificity: 73%).

SPARCL1 as a predictor of early maladaptive remodelling

In the IPAH group, NT-proBNP and SPARCL1 were analysed as predictors of early maladaptive remodelling. NT-proBNP and SPARCL1 levels were higher in IPAH patients with Ees/Ea < 1.5 ($P < 0.001$ for both comparisons, *Figure* 4A,B) and RVESVI > 31 mL/m^2 ($P < 0.001$ for SPARCL1 and P = 0.005 for NT-proBNP, *Figure* 4C,D). SPARCL1 levels were also higher in IPAH patients with RVEF < 50% (P = 0.005,

Table 2 Clinical characteristics of patients grouped according to adaptive or maladaptive remodelling.

	IPAH		
	Adaptive RV remodelling $n = 52$	Maladaptive RV remodelling $n = 21$	*P* value
Age, years, median (IQR)	69 (56–74)	71 (61–81)	0.064
BMI, kg/m^2, median (IQR)	28 (25–32)	25 (23–31)	0.147
BSA, m^2, median (IQR)	1.95 (1.83–2.16)	1.84 (1.73–2.02)	0.093
Female sex, *n* (%)	17 (33%)	9 (43%)	0.412
NYHA ≥ III, *n* (%)	26 (52%)	14 (70%)	0.169
Arterial hypertension, *n* (%)	27 (52%)	10 (48%)	0.739
Diabetes, *n* (%)	4 (8%)	5 (24%)	0.063
Hypercholesterolemia, *n* (%)	4 (8%)	3 (14%)	0.402
COPD, *n* (%)	5 (10%)	3 (14%)	0.563
CAD, *n* (%)	4 (8%)	5 (24%)	0.058
Stroke, *n* (%)	1 (2%)	1 (5%)	0.501
Right heart catheterization			
PASP, mmHg, median (IQR)	39 (30–64)	79 (61–88)	0.000
PCWP, mmHg, median (IQR)	10 (7–12)	11 (9–14)	0.209
PVR, dyn s cm^{-5}, median (IQR)	219 (136–414)	573 (407–782)	0.000
mPAP, mmHg, median (IQR)	25 (19–37)	46 (37–52)	0.000
CI, L/min/m^2, median (IQR)	2.71 (2.48–3.14)	2.37 (1.98–2.77)	0.015
RAP, mmHg, median (IQR)	6 (5–9)	9 (6–12)	0.087
PV loop measurements			
RV EDP, mmHg, median (IQR)	6 (3–8)	10 (6–14)	0.002
RV ESP, mmHg, median (IQR)	38 (24–51)	64 (50–84)	0.000
SW, mmHg mL m^{-2}, median (IQR)	2091 (1273–2676)	2098 (1952–3775)	0.043
Tau, ms, median (IQR)	32 (28–40)	37 (34–43)	0.008
dP/dt min, mmHg/s, median (IQR)	−341 (−525 to −241)	−541 (−610 to −473)	0.001
dP/dt max, mmHg/s, median (IQR)	376 (284–440)	429 (335–518)	0.050
Eed, mmHg/mL, median (IQR)	0.16 (0.11–0.23)	0.30 (0.23–0.37)	0.000
Ees, mmHg/mL, median (IQR)	0.68 (0.46–0.94)	0.75 (0.60–0.99)	0.257
Ees/Ea ratio, median (IQR)	1.37 (1.06–1.56)	0.84 (0.68–1.01)	0.000
Echocardiography			
LVEF, %, median (IQR)	59 (55–62)	58 (54–61)	0.568
TAPSE, mm, median (IQR)	22 (20–24)	15 (14–19)	0.000
TAPSE/PASP, mm/mmHg, median (IQR)	1 (0–1)	0 (0–0)	0.000
RA, cm^2, median (IQR)	17 (13–21)	27 (19–31)	0.000
S′, cm/s, median (IQR)	11 (10–14)	9 (8–12)	0.002
RVEDd, mm, median (IQR)	44 (40–49)	52 (45–58)	0.000
FAC, %, median (IQR)	40 (33–44)	28 (26–31)	0.000
TI_qual_0_1l_2m_3 (mean)	1	2	0.000
RVstrain_fw, median (IQR)	−24 (−27 to −21)	−15 (−20 to −13)	0.000
RVstrain_4k, median (IQR)	−20 (−23 to −19)	−14 (−18 to −12)	0.000
3D echocardiography			
LVEDV, mL, median (IQR)	127 (105–160)	96 (83–129)	0.004
LVESV, mL, median (IQR)	53 (41–65)	40 (34–50)	0.016
RVESVI, mL/m^2, median (IQR)	33 (24–41)	57 (42–67)	0.000
RVSVI, mL/m^2, median (IQR)	27 (23–32)	27 (23–30)	0.323
RVEF, %, median (IQR)	45 (41–51)	32 (27–37)	0.000
Biomarkers			
SPARCL1, ng/mL, median (IQR)	2.34 (1.80–5.35)	5.91 (3.83–9.22)	0.003
NT-proBNP, pg/mL, median (IQR)	171 (64–694)	992 (268–2346)	0.001
eGFR, mL/min, median (IQR)	90 (70–106)	60 (46–71)	0.000
PAH drugs			
PDE5, *n* (%)	2 (4%)	1 (5%)	0.858
ERA, *n* (%)	3 (6%)	1 (5%)	0.864
sGC, *n* (%)	3 (6%)	3 (14%)	0.230
PCI, *n* (%)	1 (2%)	1 (5%)	0.501

Abbreviations: BMI, body mass index; CAD, coronary artery disease; CI, cardiac index; COPD, chronic obstructive pulmonary disease; Eed, end-diastolic elastance; Ees, end-systolic elastance; eGFR, estimated glomerular filtration rate; ERA, endothelin receptor antagonists; FAC, fractional area change; IQR, interquartile range; IVSd, interventricular septum diastolic diameter; LVEDd, left ventricular end-diastolic diameter; LVEF, left ventricular ejection fraction; LVPWd, left ventricular posterior wall diastolic diameter; MI, myocardial infarction; mPAP, mean pulmonary arterial pressure; NT-proBNP, N-terminal pro-brain natriuretic protein; NYHA, New York Heart Association; PASP, systolic pulmonary artery pressure; PCWP, pulmonary capillary wedge pressure; PDE5, phosphodiesterase-5 inhibitors; PV, pulmonary vein; PVR, pulmonary vein resistance; RA area, right atrial; RAP, right atrial pressure; RV EDA, right ventricular end-diastolic area; RV EDP, right ventricular end-diastolic pressure; RV ESA, right ventricular end-systolic area; RV ESP, right ventricular end-systolic pressure; RVEDd, right ventricular end-diastolic diameter; RVEDV, right ventricular end-diastolic volume; RVEDVI, right ventricular end-diastolic volume index; RVEF, right ventricular ejection fraction; RVESV, right ventricular end-systolic volume index; RVESVI, right ventricular end-systolic volume index; RVFWS, right ventricular free wall strain; RVGLS, right ventricular global longitudinal strain; RVSVI, right ventricular stroke volume index; sGC, soluble guanylate cyclase stimulators; SPARCL1, SPARC-like protein 1; SW, stroke work; TAPSE, tricuspid annular plane systolic excursion.

Figure 2 Plasma biomarker levels in patients in adaptive and maladaptive RV remodelling versus controls. (A) NT-proBNP levels. (B) SPARCL1 levels. *$P < 0.05$; **$P < 0.01$; ***$P < 0.001$; ****$P < 0.0001$. NT-proBNP, N-terminal pro-brain natriuretic protein; RV, right ventricle; SPARCL1, SPARC-like protein 1.

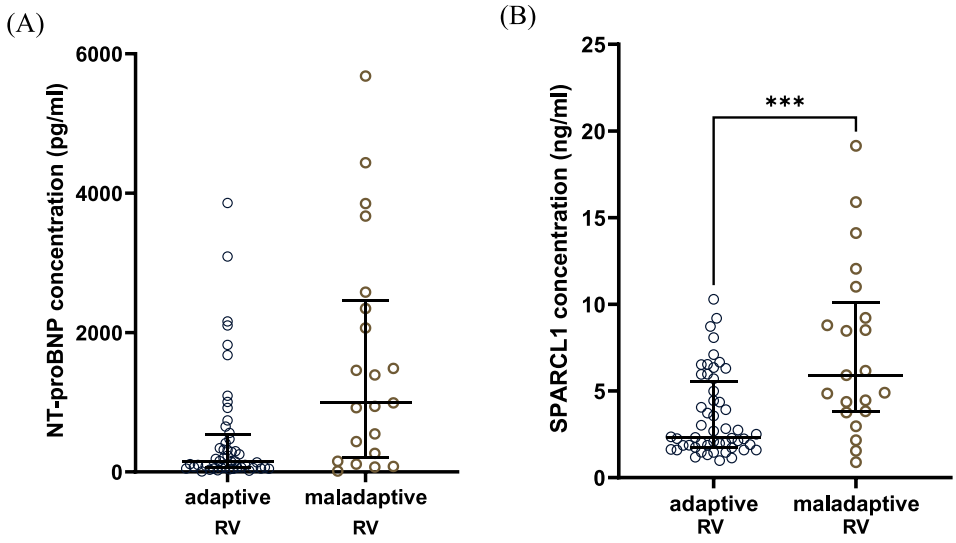

Figure 4E), whereas there were no significant differences between NT-proBNP levels in IPAH patients with RVEF $< 50\%$ and RVEF $> 50\%$ ($P = 0.08$, *Figure* 4F).

ROC curve analysis in all IPAH patients showed a tendency for a better predictive value of SPARCL1 than NT-proBNP in terms of early maladaptive changes defined as: Ees/Ea < 1.5 ($AUC_{SPARCL1} = 0.84$, $AUC_{NT\text{-}proBNP} = 0.81$, $P = 0.5$ for $AUC_{SPARCL1}$ vs. $AUC_{NT\text{-}proBNP}$, Figure S3A), RVESVI > 31 mL/m^2 ($AUCS_{PARCL1} = 0.78$, $AUC_{NT\text{-}proBNP} = 0.71$, $P = 0.10$ for $AUC_{SPARCL1}$ vs. $AUC_{NT\text{-}proBNP}$, Figure S3B), RVEDd > 42 mm. ($AUC_{SPARCL1} = 0.72$, $AUC_{NT\text{-}proBNP} = 0.65$, $P = 0.19$ for $AUC_{SPARCL1}$ vs. $AUC_{NT\text{-}proBNP}$, Figure S3C) and RVEF $< 50\%$ ($AUC_{SPARCL1} = 0.77$, $AUC_{NT\text{-}proBNP} = 0.67$, $P = 0.07$ for $AUC_{SPARCL1}$ vs. $AUC_{NT\text{-}proBNP}$, Figure S3D).

Discussion

The main findings of this study are[1] as follows: SPARCL1 and NT-proBNP are similarly correlated with invasive PV loop parameters of RV contractility, diastolic function and RV–PA coupling as well as with 3D echocardiographic parameters of RV systolic function and dilation in IPAH patients[2]; SPARCL1 and NT-proBNP are good predictors of RV–PA uncoupling and maladaptive RV remodelling, and combined, they have an improved predictive power for maladaptive RV remodelling[3]; parameters of early RV maladaptation show a better association with increased SPARCL1 levels than with increased NT-proBNP levels.

RV function is the major predictor of morbidity and mortality in patients with PH.[3] Chronic pressure overload leads to maladaptive RV remodelling that is associated with progressive systolic and diastolic dysfunction. Eventually, the RV can no longer compensate for the increased afterload, which results in RV–PA uncoupling.[2] The precise measurement of RV contractile and relaxation properties as well as RV–PA coupling is challenging. Parameters measured by non-invasive echocardiography and cardiac magnetic resonance are load dependent, and right heart catheterization is an invasive diagnostic tool that mainly provides pressure measurements.[15] PV loop analysis is the gold standard for load-independent measurements of systolic and diastolic RV function and RV–PA coupling that can provide the most accurate assessment of intrinsic RV changes caused by maladaptive RV remodelling. Recent technical advances have made reliable PV loop measurements possible in the clinical setting. Nevertheless, evidence for associations between biomarker concentrations and PV loop parameters is still scarce.

NT-proBNP is an established biomarker of RV dysfunction and prognosis in patients with PH. It is an essential component of risk stratification in PH, and it is included in the REVEAL risk score[16] that assesses mortality in PAH and in the three-strata model of the ESC/ERS guidelines for one-year mortality in patients with PH.[3]

The expression of the matricellular protein SPARCL1, a member of the SPARC family of proteins, has been shown to increase in experimental models of LV hypertrophy and fibrosis.[17] SPARCL1 expression was higher in an experimental rat model of maladaptive RV hypertrophy with monocrotaline-induced PH.[7] In a previously published pilot study,[8] our research team identified SPARCL1 as a potential biomarker of maladaptive RV remodelling in PH. High SPARCL1 levels were associated with echocardiographic

Figure 3 Receiver operating characteristics curve showing the predictive power of SPARCL1, NT-proBNP and the combined predictive power of SPARCL1 and NT-proBNP for maladaptive RV remodelling. NT-proBNP, N-terminal pro-brain natriuretic protein; RV, right ventricle; SPARCL1, SPARC-like protein 1.

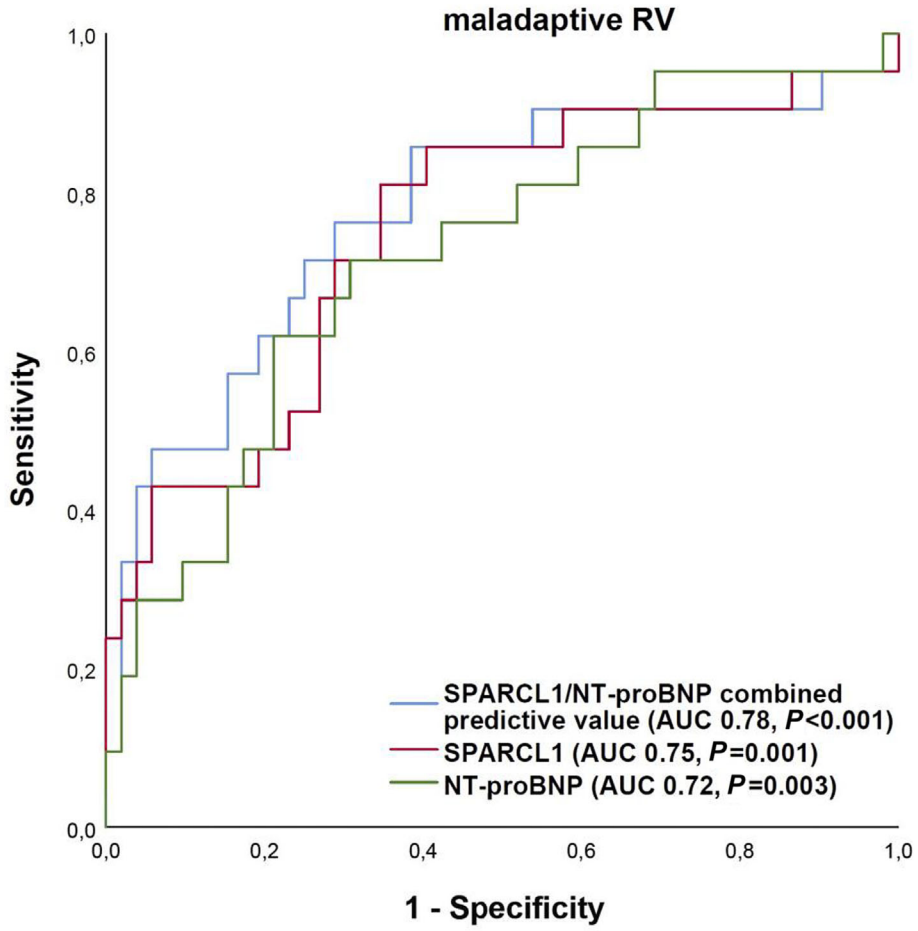

parameters of systolic dysfunction and RV dilatation as well as with low TAPSE/PASP, a non-invasive parameter of RV–PA coupling. However, the assessment of RV function and pulmonary circulation in this pilot study was based only on echocardiography and right heart catheterization,[8] which does not allow a load-independent evaluation of RV physiology and RV–PA coupling.

In the present study, NT-proBNP and SPARCL1 showed a similar performance in terms of association and correlation with invasive PV loop parameters as well as echocardiographic parameters. Both biomarkers were moderately correlated with invasive PV loop parameters of systolic and diastolic RV function and RV–PA coupling.

NT-proBNP and SPARCL1 showed a moderate positive correlation with Ees, which is a load-independent parameter of RV contractility. A four- to four-fold increase in Ees during the early phase of PH is one of the most adaptive responses of the RV to the increased afterload. Even though the intrinsic RV contractile properties deteriorate during maladaptive RV remodelling in patients with PH, RV contractility remains higher than in healthy patients, even after uncoupling occurs.[18] This is the most probable explanation for the positive correlation of NT-proBNP and SPARCL1 levels with Ees. However, higher NT-proBNP and SPARCL1 levels also correlated with overall diastolic dysfunction (higher Tau) and higher diastolic stiffness (higher Eed).

Eed and Tau have been identified as important parameters of RV maladaptation. Studies show that diastolic dysfunction and stiffness are associated with increased RV fibrosis, which consists of sarcomeric changes in cardiomyocytes that lead to impaired lusitropic RV function.[14,19] Progressive diastolic dysfunction also seems to be a crucial maladaptive mechanism in the transition to RV–PA uncoupling in PH patients.[20]

Most importantly, higher NT-proBNP and SPARCL1 levels were also associated with lower Ees/Ea, which is the current gold standard for determining RV/PA uncoupling. Pulmonary arterial elastance (Ea) reflects both resistive and pulsatile

Figure 4 (A) NT-proBNP levels in IPAH patients with Ees/Ea $<$ 1.5 versus Ees/Ea $\geq$ 1.5. (B) SPARCL1 levels in IPAH patients with Ees/Ea $<$ 1.5 versus Ees/Ea $\geq$ 1.5. (C) NT-proBNP levels in IPAH patients with RVESVI $<$ 31 mL/m^2 versus $\geq$31 mL/m^2. (D) SPARCL1 levels in IPAH patients with RVESVI $<$ 31 mL/m^2 versus $\geq$31 mL/m^2. (E) NT-proBNP levels in IPAH patients with RVEF $\leq$ 50% versus $>$50%. (F) SPARCL1 levels in IPAH patients with RVEF $\leq$ 50% versus $>$50%. ns, not significant; $^{**}P < 0.01$; $^{***}P < 0.001$; $^{****}P < 0.0001$.

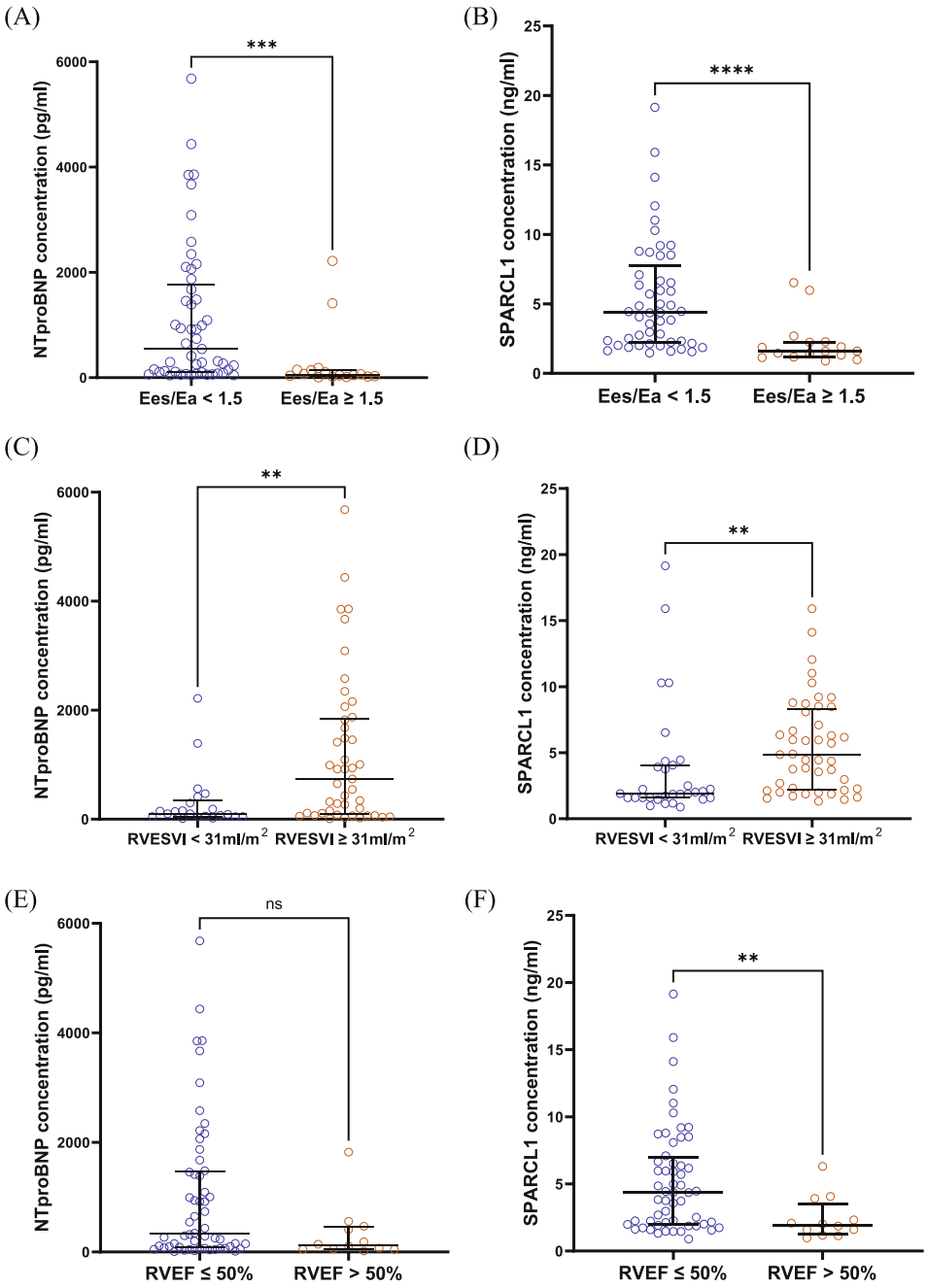

components of RV afterload, which allows its exact measurement. Hence, Ees/Ea refers to the relationship between RV contractility and RV afterload. All parameters of RV output obtained from echocardiography, right heart catheterization and MRI such as TAPSE, RVEF and CI are influenced by the current volume status of the patient, whereas Ees/Ea is a load-independent parameter. It continually decreases following maladaptive changes in the RV under increasing pressure overload until the point of uncoupling is reached. At that point, the RV cannot maintain a sufficient cardiac output, which leads to right heart failure. Ees/Ea $<$ 0.8 has been identified as a cut-off for RV–PA uncoupling that is also associated

DOI: 10.1002/ehf2.15159

with increased mortality, and Ees/Ea $<$ 1.1 was associated with clinical worsening.[21,22]

There is no established definition of adaptive and maladaptive RV remodelling. Hence, the prognostic three-strata risk model of the ESC/ERS guidelines for PH, based on validated determinants for 1 year mortality, was used for the definition of adaptive and maladaptive RV remodelling in this study. This classification was further modified by adding Ees/Ea $<$ 1.1 as an additional feature of RV maladaptation. The clinical characteristics of the maladaptive RV group clearly demonstrate a maladaptive phenotype with systolic RV dysfunction, RV dilation, RV–PA uncoupling and an intermediate (5%–20%) to high ($>$20%) risk of 1 year mortality, whereas the clinical features of the IPAH patients from the group with adaptive RV remodelling categorize them in the low ($<$5%) to intermediate risk for 1 year mortality.

The plasma levels of NT-proBNP and SPARCL1 were significantly higher in the maladaptive group, and ROC analysis revealed that they were both good predictors of maladaptive RV remodelling. The combined predictive value of the two biomarkers had an improved sensitivity and specificity for maladaptive RV than either biomarker alone. Therefore, the use of both NT-proBNP and SPARCL1 in a panel of biomarkers could be advantageous in diagnosing maladaptive RV remodelling. Furthermore, SPARCL1 seems to have additional value for the prediction of early maladaptation as compared with NT-proBNP.

Limitations

This is a single-centre study of observational nature. The sample size was small, which could limit the validity of our analyses. Furthermore, it is possible that SPARCL1 levels are influenced by the pulmonary vascular remodelling associated with IPAH. However, evidence on SPARCL1 is scarce, and to the best of our knowledge, there are no studies that have analysed SPARCL1 expression in pulmonary cells of patients with PH. SPARCL1 and NT-proBNP levels could have been influenced by worse renal function in patients with maladaptive RV remodelling, although the renal filtration rate as measured by eGFR was only mildly reduced.

Conclusions

NT-proBNP and SPARCL1 plasma levels were similarly correlated with invasive load-independent parameters of RV systolic/diastolic function and RV–PA-coupling in IPAH patients. Furthermore, they were both good predictors of prognostically relevant RV maladaptation. Further research is needed to analyse the potential of SPARCL1 as a biomarker of early maladaptive RV remodelling.

Acknowledgements

We acknowledge the expertise of Elizabeth Martinson, PhD, of the KHFI Editorial Office in preparing the manuscript.

Open Access funding enabled and organized by Projekt DEAL.

[Correction added on 16 December 2024, after first online publication: Projekt DEAL funding statement has been added.]

Conflict of interest

The authors report no conflict of interest.

Financial disclosures

Project B07, Collaborative Research Center 1213-Pulmonary Hypertension and Cor Pulmonale, German Research Foundation (DFG). The authors have no financial relationships with industry or other entities pertaining to the subject of this manuscript.

Data availability statement

The data that support the findings of this study are available from the corresponding author, S. K., upon reasonable request.

Supporting information

Additional supporting information may be found online in the Supporting Information section at the end of the article.

Figure S1. Correlation plots showing correlations between: (1) Ees and NT-proBNP levels. (J) Ees and SPARCL1 levels. (K) Eed and NT-proBNP levels. (L) Eed and SPARCL1 levels. (M) Tau and NT-proBNP levels. (N) Tau and SPARCL1 levels. (O) Ees/Ea and NT-proBNP levels. (P) Ees/Ea and SPARCL1 levels.
Figure S2. Parameters of RV function and RV–PA coupling in patients with adaptive and maladaptive RV remodelling. (J) mPAP. (K) Ees/Ea. (L) TAPSE/PASP. (M) Ees. (N) RVEF. (O) Eed. (P) Tau. (Q) RVESVI. (R) Representative PV loops for patients with (A) adaptive and (B) maladaptive RV remodelling.
Figure S3. Receiver operating characteristics curve showing the predictive power of SPARCL1 and NT-proBNP for: (E) RVEDD $>$ 42 mm. (F) RVESVI $>$ 31 mL/m^2. (G) Ees/Ea $<$ 1.5. (H) RVEF $<$ 50%.

References

1. Tello K, Seeger W, Naeije R, Vanderpool R, Ghofrani HA, Richter M, Tedford RJ, Bogaard HJ Right heart failure in pulmonary hypertension: diagnosis and new perspectives on vascular and direct right ventricular treatment. *Br J Pharmacol* 2021;**178**:90–107. doi:10.1111/bph.14866.
2. Vonk Noordegraaf A, Chin KM, Haddad F, Hassoun PM, Hemnes AR, Hopkins SR, Kawut SM, Langleben D, Lumens J, Naeije R Pathophysiology of the right ventricle and of the pulmonary circulation in pulmonary hypertension: an update. *Eur Respir J* 2019;**53**:1801900. doi:10.1183/13993003.01900-2018
3. Humbert M, Kovacs G, Hoeper MM, Badagliacca R, Berger RMF, Brida M, Carlsen J, Coats AJS, Escribano-Subias P, Ferrari P, Ferreira DS, Ghofrani HA, Giannakoulas G, Kiely DG, Mayer E, Meszaros G, Nagavci B, Olsson KM, Pepke-Zaba J, Quint JK, Rådegran G, Simonneau G, Sitbon O, Tonia T, Toshner M, Vachiery JL, Vonk Noordegraaf A, Delcroix M, Rosenkranz S, ESC/ERS Scientific Document Group, Schwerzmann M, Dinh-Xuan AT, Bush A, Abdelhamid M, Aboyans V, Arbustini E, Asteggiano R, Barberà JA, Beghetti M, Čelutkienė J, Cikes M, Condliffe R, de Man F, Falk V, Fauchier L, Gaine S, Galié N, Gin-Sing W, Granton J, Grünig E, Hassoun PM, Hellemons M, Jaarsma T, Kjellström B, Klok FA, Konradi A, Koskinas KC, Kotecha D, Lang I, Lewis BS, Linhart A, Lip GYH, Løchen ML, Mathioudakis AG, Mindham R, Moledina S, Naeije R, Nielsen JC, Olschewski H, Opitz I, Petersen SE, Prescott E, Rakisheva A, Reis A, Ristić AD, Roche N, Rodrigues R, Selton-Suty C, Souza R, Swift AJ, Touyz RM, Ulrich S, Wilkins MR, Wort SJ 2022 ESC/ERS guidelines for the diagnosis and treatment of pulmonary hypertension. *Eur Heart J* 2022;**43**:3618–3731. doi:10.1093/eurheartj/ehac237
4. Chin KM, Rubin LJ, Channick R, Di Scala L, Gaine S, Galie N, et al. Association of N-terminal pro brain natriuretic peptide and long-term outcome in patients with pulmonary arterial hypertension. *Circulation* 2019;**139**:2440–2450. doi:10.1161/CIRCULATIONAHA.118.039360
5. Lewis RA, Durrington C, Condliffe R, Kiely DG. BNP/NT-proBNP in pulmonary arterial hypertension: time for point-of-care testing? *European Respiratory Review: An Official Journal of the European Respiratory Society* 2020;**29**:200009. doi:10.1183/16000617.0009-2020
6. Sullivan MM, Barker TH, Funk SE, Karchin A, Seo NS, Hook M, et al. Matricellular hevin regulates decorin production and collagen assembly. *J Biol Chem* 2006;**281**:27621–27632. doi:10.1074/jbc.M510507200
7. Imoto K, Okada M, Yamawaki H. Expression profile of matricellular proteins in hypertrophied right ventricle of monocrotaline-induced pulmonary hypertensive rats. *J Vet Med Sci* 2017;**79**:1096–1102. doi:10.1292/jvms.17-0053
8. Keranov S, Dörr O, Jafari L, Liebetrau C, Keller T, Troidl C, Kriechbaum S, Voss S, Richter M, Tello K, Gall H, Ghofrani HA, Mayer E, Seeger W, Hamm CW, Nef H SPARCL1 as a biomarker of maladaptive right ventricular remodelling in pulmonary hypertension. *Biomarkers: biochemical indicators of exposure, response, and susceptibility to chemicals* 2020;**25**:290–295. doi:10.1080/1354750X.2020.1745889
9. Gall H, Felix JF, Schneck FK, Milger K, Sommer N, Voswinckel R, Franco OH, Hofman A, Schermuly RT, Weissmann N, Grimminger F, Seeger W, Ghofrani HA The Giessen Pulmonary Hypertension Registry: survival in pulmonary hypertension subgroups. *J Heart Lung Transpl* 2017;**36**:957–967. doi:10.1016/j.healun.2017.02.016
10. Recommendations for cardiac chamber quantification by echocardiography in adults: an update from the American Society of Echocardiography and the European Association of, Cardiovascular Imaging. *Eur Heart J Cardiovasc Imaging* 2016;**17**:412. doi:10.1093/ehjci/jew041
11. Rosenkranz S, Preston IR. Right heart catheterisation: best practice and pitfalls in pulmonary hypertension. *Eur Respir Rev* 2015;**24**:642–652. doi:10.1183/16000617.0062-2015
12. Brimioulle S, Wauthy P, Ewalenko P, Rondelet B, Vermeulen F, Kerbaul F, et al. Single-beat estimation of right ventricular end-systolic pressure–volume relationship. *Am J Physiol Heart Circ Physiol* 2003;**284**:H1625–H1630. doi:10.1152/ajpheart.01023.2002
13. Trip P, Rain S, Handoko ML, van der Bruggen C, Bogaard HJ, Marcus JT, Boonstra A, Westerhof N, Vonk-Noordegraaf A, de Man FS Clinical relevance of right ventricular diastolic stiffness in pulmonary hypertension. *Eur Respir J* 2015;**45**:1603–1612. doi:10.1183/09031936.00156714
14. Rain S, Handoko ML, Trip P, Gan CT, Westerhof N, Stienen GJ, et al. Right ventricular diastolic impairment in patients with pulmonary arterial hypertension. *Circulation* 2013;**128**:2016–25, 1–10, 2025. doi:10.1161/CIRCULATIONAHA.113.001873
15. Brener MI, Masoumi A, Ng VG, Tello K, Bastos MB, Cornwell WK, III, et al. Invasive right ventricular pressure–volume analysis: basic principles, clinical applications, and practical recommendations. *Circ Heart Fail* 2022;**15**:e009101. doi:10.1161/CIRCHEARTFAILURE.121.009101
16. Galie N, Channick RN, Frantz RP, Grunig E, Jing ZC, Moiseeva O, et al. Risk stratification and medical therapy of pulmonary arterial hypertension. *Eur Respir J* 2019;**53**:1801889. doi:10.1183/13993003.01889-2018
17. Frangogiannis NG. Matricellular proteins in cardiac adaptation and disease. *Physiol Rev* 2012;**92**:635–688. doi:10.1152/physrev.00008.2011
18. Noordegraaf AV, Westerhof BE, Westerhof N. The relationship between the right ventricle and its load in pulmonary hypertension. *J Am Coll Cardiol* 2017;**69**:236–243. doi:10.1016/j.jacc.2016.10.047
19. Rain S, Andersen S, Najafi A, Gammelgaard Schultz J, da Silva Goncalves Bos D, Handoko ML, et al. Right ventricular myocardial stiffness in experimental pulmonary arterial hypertension: relative contribution of fibrosis and myofibril stiffness. Circulation *Heart failure* 2016;**9**. doi:10.1161/CIRCHEARTFAILURE.115.002636
20. Tello K, Dalmer A, Vanderpool R, Ghofrani HA, Naeije R, Roller F, Seeger W, Wilhelm J, Gall H, Richter MJ Cardiac magnetic resonance imaging-based right ventricular strain analysis for assessment of coupling and diastolic function in pulmonary hypertension. *J Am Coll Cardiol Img* 2019;**12**:2155–2164. doi:10.1016/j.jcmg.2018.12.032
21. Tello K, Dalmer A, Axmann J, Vanderpool R, Ghofrani HA, Naeije R, Roller F, Seeger W, Sommer N, Wilhelm J, Gall H, Richter MJ Reserve of right ventricular-arterial coupling in the setting of chronic overload. *Circ Heart Fail* 2019;**12**:e005512. doi:10.1161/CIRCHEARTFAILURE.118.005512
22. Axell RG, Messer SJ, White PA, McCabe C, Priest A, Statopoulou T, Drozdzynska M, Viscasillas J, Hinchy EC, Hampton-Till J, Alibhai HI, Morrell N, Pepke-Zaba J, Large SR, Hoole SP Ventriculo-arterial coupling detects occult RV dysfunction in chronic thromboembolic pulmonary vascular disease. *Physiol Rep* 2017;**5**:e13227. doi:10.14814/phy2.13227